Acta Biochimica Polonica

Vol. 44 No. 3/1997

607–624

QUARTERLY

Conformations, orientations and time scales characterising dimyristoylphosphatidylcholine bilayer membrane. Molecular dynamics simulation studies*

Marta Pasenkiewicz-Gierula✉ and Tomasz Róg

Department of Biophysics, Institute of Molecular Biology, Jagiellonian University, Cracow, Poland

Key words: L-α-dimyristoylphosphatidylcholine bilayer membrane, membrane dynamics, membrane dynamical structure, MD simulation

The results of molecular dynamics simulation of fully hydrated dimyristoylphosphatidylcholine (DMPC) bilayer membrane in the liquid-crystalline phase are presented. They show that the probability of a *gauche* conformation varies periodically along the chain with only a slight increase towards the end of the chain. However, the frequency of transition between conformations increases, due to a decrease in the lifetime of the *trans* conformation, along the chain. The average lifetimes for *trans* conformations are in the range of $1–2 \times 10^{-10}$ s and for *gauche* conformations in the range of $4–7 \times 10^{-11}$ s. The α-chain of the DMPC head group has mainly an extended conformation, due to predominantly *trans* conformation of α5 torsion. The rotational correlation time for the P–N vector is 3.7 ns. The C2–C1–O11–P fragment of the DMPC head group (θ1, α1, α2 torsions) is rigid while the P–O12–C11–C12 fragment (α3, α4, α5 torsions) is flexible. The lateral diffusion coefficient for DMPC self-diffusion in the membrane is 2×10^{-7} cm²/s; the rate of transverse diffusion is the same. Large differences in the calculated rotational correlation times for the α-, β-, γ-chains and for the O21–C1 vector indicate that in the liquid-crystalline bilayer each segment of the DMPC molecule exhibits its own rotational freedom, in addition to its internal flexibility resulting from rotational isomerism. The results obtained in these calculations, although in general agreement with some experimental data, shed new light on the dynamical behaviour of phosphatidylcholine molecules in the bilayer membrane in the liquid-crystalline phase.

The functioning of biological membranes is, to a large extent, determined by the structure and dynamics of their liquid-crystalline matrices. The matrix is a bilayer made up of amphiphilic lipid molecules. Many properties common to all biological membranes can be learned and understood by studying the bilayers (model membranes). As phospholipids are the most common component of the matrix of plasma membranes, they are often

*This work was partially supported by a grant from The Polish Science Foundation (BIMOL 103/93)

✉Corresponding author: Department of Biophysics, Institute of Molecular Biology, Jagiellonian University, al. A. Mickiewicza 3, 31-120 Kraków, Poland. Tel: (+48-12)-34-13-05; Fax: (+48-12)-33-69-07; E-mail: mpg@mol.uj.edu.pl

Abbreviations: PC, phosphatidylcholine; DMPC, dimyristoylphosphatidylcholine; DPPC, dipalmitoylphosphatidylcholine; EPC, egg phosphatidylcholine; DPC, didihydrosterculoylphosphatidylcholine; MD, molecular dynamics; RAF, reorientational autocorrelation function; MSD, mean square displacement.

used as a single or main component of model bilayer membranes. In this paper only phosphatidylcholine (PC) model membranes are discussed.

Experimental studies, mainly using electron paramagnetic resonance (EPR), nuclear magnetic resonance (NMR), fluorescence, infra-red and Raman spectroscopies, show that a model membrane in the liquid-crystalline phase is characterised by a large structural disorder. In contrast to the crystal structure, where hydrocarbon chains assume all-*trans* conformation, the average number of *gauche* conformations is about 3 in the 14-carbon atoms alkyl chain [1, 2] and increases with increasing chain length [1, 3]. In the membrane, lipid molecules exhibit unhindered rotational diffusion around their long axes together with fluctuations of the long axis relative to the membrane normal (hindered rotation around the axis perpendicular to the long axis) [4]. They can also move in the plane of the membrane [5, 6], and, in a limited range, in the plane normal to it [7]. Any longer range order, present in the crystalline phase, is lost in the liquid-crystalline phase as a result of these conformational and diffusional changes.

There is a wide range of time scales of dynamic processes involving membrane phospholipids and their fragments. Except for the bond oscillations and angle vibrations, the shortest is *trans-gauche* isomerism of torsion angles in the hydrocarbon chains, which is of the order of 10^{-10} s [8]. The longest, with correlation times longer than 10^{-4} s, is associated with collective movements of the lipid molecules and undulations observed in the cell plasma membranes [9].

Experimental studies of membrane structure and dynamics are difficult to interpret because of the structural disorder and superposition of motions occurring in different time scales. Besides, due to limited spatial and time resolutions, they provide only an averaged behaviour of the molecular motions for the characteristic experimental time window.

Detailed information about the dynamic structure and time scales of events in the membrane can be obtained using molecular dynamics (MD) simulation methods. Although MD simulation is characterised by an atomic resolution and time resolution in the femtosecond time scale in principle, the total simulation time is limited at present to several nanoseconds. So, the method allows observation of the processes up to the 10^{-8} s time scale.

In this paper we analyse the equilibrium structure and dynamics of fully hydrated dimyristoylphosphatidylcholine (DMPC) bilayer membrane in the liquid-crystalline phase simulated for over 4.5 ns. We have determined time scales of conformational, orientational and positional changes of groups of atoms and of whole molecules in the membrane. Whenever possible, we compared our results with published experimental data.

METHODS

Simulation system. A DMPC bilayer membrane consisting of 72 ($6 \times 6 \times 2$) DMPC molecules and 1622 water molecules was used. The membrane was simulated for over 4500 ps using AMBER 4.0 [10]. The starting configuration was the minimised structure of Vanderkooi in the second arrangement [11]. Figure 1 shows the structure, numbering of atoms and torsion angles in the DMPC molecule. The system was equilibrated for 1100 ps. Details concerning the membrane construction and equilibration are described in Ref. [12].

Simulation parameters. Parameters of optimised potentials for liquid simulations (OPLS) [13] for DMPC and TIP3P in water were used [14]. The united atom approximation was applied to the DMPC molecule to reduce computation time. The atomic charges of the DMPC molecule used in this simulation are given in Ref. [12].

Simulation conditions. The SHAKE algorithm [15] was used to preserve the bond lengths of the water molecule and the time step was set at 2 fs [16]. For non-bonded interactions, a residue-based cutoff was employed with a cutoff distance of 12 Å. To reduce calculation time of non-bonded interactions each DMPC was divided into 6 residues. Each residue was chosen in such a way

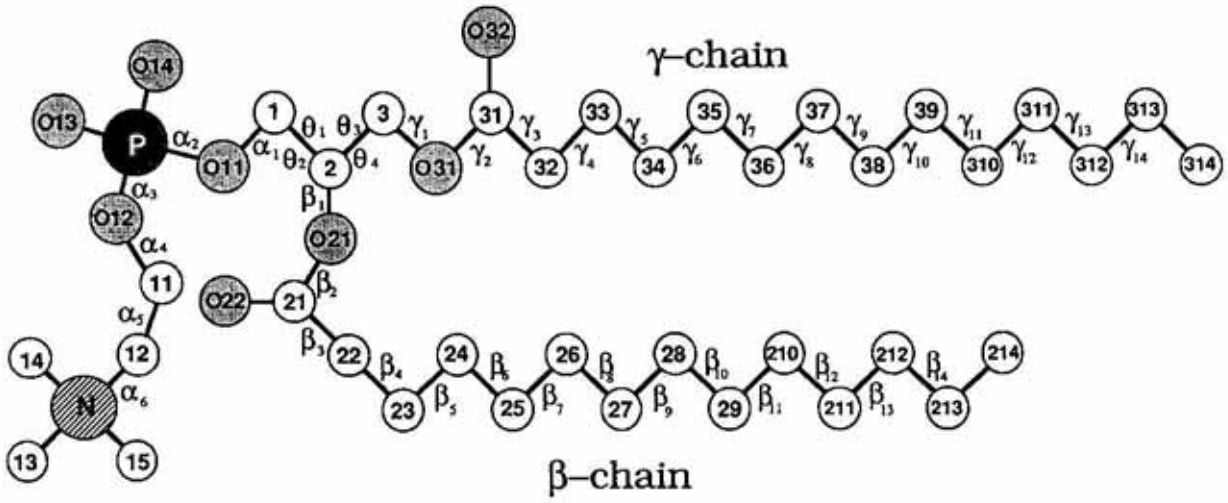

Figure 1. Atom numbering and notation for torsion angles in the DMPC molecule.

that the total electrostatic charge on the residue was close to zero and the integrity of its chemical groups was preserved [12]. The list of non-bonded pairs was updated every 50 steps.

Simulation was carried out at a constant pressure of 1 atm and a constant temperature of 310 K (37°C), which is above the main phase transition temperature for the DMPC bilayer (approx. 23°C). The temperatures of the solute and solvent were controlled independently: the Berendsen method [17] was used to control the temperatures and pressure of the system. The relaxation times for temperatures and pressure were set at 0.4 and 0.6 ps, respectively. The applied pressure was controlled anisotropically, where each direction was treated independently and the trace of the pressure tensor was kept constant (1 atm). Three-dimensional periodic boundary conditions employing the usual minimum image convention were used. Due to the employed pressure control the dimensions of the periodic box changed during the simulation. After equilibration, they were 32.4, 67.0, 56.7 Å and at the end of simulation 35.7, 60.0, 57.6 Å, in the x, y and z-direction, respectively.

Calculations of the dynamic properties. The reorientational autocorrelation function (RAF) was calculated at discrete time steps according to:

$$C_l(\tau) = < P_l(n(t_0) \cdot n(t_0 + \tau) > t_0 \qquad (1)$$

where P_l is the l-th Legendre polynomial, n is a fixed unit vector in the molecule, t_0 and τ are the initial and lap times, respectively, and $<\ldots>t_0$ denotes an averaging over different initial times within a simulation run and over all molecules in the system. This correlation function usually decays exponentially with time. Its rates of decay are here (as in optical spectroscopy) called correlation times, however, in NMR spectroscopy the correlation time is the integral of the correlation function C_2 (in the case of single exponential decay both definitions coincide). In this paper the correlation times were obtained from a fit of C_1 and C_2 to a sum of two to four exponentials:

$$C_l = \sum_{i=1}^{n} a_i^l \exp(-t/\tau_i^l) \qquad (2)$$

where τ_i^l is the i-th correlation time, a_i^l is the i-th pre-exponential factor (amplitude) (related to the contribution of the i-th decay process to the total decay), for the l-th Legendre polynomial, and n is the number of exponentials (n = 2, 3 or 4). In each case, the smallest number of exponentials necessary to fit a given RAF was used.

The mean square displacement (MSD) at discrete time steps is given by:

$$MSD(\tau) = < | r(t_0) - r(t_0 + \tau) |^2 > t_0 \qquad (3)$$

where r is the position of the molecule, t_0 and τ are the initial and lap times, respectively, and $<...>_{t_0}$ denotes an averaging over different initial times within a simulation run and over all molecules in the system. From the Einstein relation the self-diffusion coefficient D can be obtained by

$$D = \lim_{t \to \infty} \frac{MSD}{2N_f t} \tag{4}$$

where N_f is the number of degrees of translational freedom for the molecule and MSD is given by equation 3.

RESULTS

We have determined various structural and dynamic characteristics of fragments of DMPC molecules as well as those of the whole molecule in the computer generated bilayer membrane. We started from analysing the two hydrocarbon chains (β- and γ-chain) and proceeded to the head group α-chain of DMPC. Finally, we have calculated the orientation and motion of the whole DMPC molecule.

The computer model membrane was simulated over a time interval of 4.5 ns. This allowed us to analyse the membrane properties during 2500 ps, that is in the time range between 2000 and 4500 ps. The details of membrane equilibration and validation of the computer model are given in Ref. [12].

Hydrocarbon chains

Conformations

The number of *gauche* conformations of torsion angles in an alkyl chain characterises the phase state of the PC bilayer. In the PC single crystal structure, all torsion angles in the chain are *trans* [18] (so called, all-*trans* conformation). Experimental studies show that, in the gel phase, the number of *gauche* conformations is 0.5 [19] and in the liquid-crystalline phase it is about 3 [1, 2, 19] for myristoyl chain (14 carbon atoms) both below and above the main phase transition temperature. In the simulated DMPC bilayer in the liquid-crystalline phase, the average number of *gauche* rotamers/myristoyl chain is 2.8 ± 0.1.

There are experimental indications that the probability of *gauche* conformation increases towards the end of the chain [20, 21]. The probabilities of *gauche*$^+$ (g^+), *trans*, and *gauche*$^-$ (g^-) rotamers along the β- and γ-chain in the simulated membrane are given in Table 1. Additionally, the probabilities of *trans*, as well as the sum of the probabilities of g^+ and g^- along the chains, are plotted in Fig. 2. The probabilities of *trans* rotamers in both chains are 3–4 times higher than those of *gauche* ones. The probability of *gauche* rotamer does not significantly increase towards the terminal methyl group in either chain, but it does show a clear oscillatory behaviour. As can be seen in Fig. 2c and d, the probability oscillations become flatter along the β-chain and in the middle of the γ-chain, mainly because of the increase of the lower side probabilities. In effect, the probability of *gauche* slightly increases (less than 17%) towards the terminal methyl group. It is interesting to notice that in the β-chain three CH_2 groups constitute the oscillation period, whereas in the γ-chain two groups. As Fig. 2a and b show, the behaviour of *trans* conformations is opposite to that of *gauche*. Large errors (standard deviations) of the calculated probabilities, of the order of 20% (Fig. 2), indicate that transitions between conformational states are not frequent.

Transitions between conformations

Populations of *trans* conformational states in the alkyl chain are 3–4 times higher than those of *gauche* states but the rotational freedom about C–C bonds in the chain allows transitions between the conformations. The calculated average transition periods for *trans* → *gauche*, *gauche* → *trans* and *gauche* → *gauche* transitions along the hydrocarbon chains are given in Table 2. The periods for *trans* → *gauche* transitions along the β- and γ-chain are also plotted in Fig. 3a and b. The periods oscillate and decrease along the chains: for the terminal torsions (β14 and

γ14) the average period is approximately shorter by a half than that for β4 and γ4. As the equilibrium number of *trans* and *gauche* conformations in the alkyl chain is preserved, the numbers of *trans* → *gauche* and *gauche* → *trans* transitions are almost equal and so are the transition periods. The latter transitions occur on the 10^{-10} s time scale, whereas *gauche* → *gauche* transitions occur on the 10^{-8} s time scale (Table 2). As can be seen in Fig. 3a and b, oscillations of the times between transitions have a period of 2 CH_2 groups and are in phase with the oscillations of the population of *trans* conformations along the γ-chain (Fig. 2b).

The transition period for each torsion is approximately the sum of the average lifetimes of its *trans* and *gauche* conformations. The lifetimes along the β- and γ-chain are given in Table 3 and those for *trans* and g^+ in Fig. 3c and d. Two selected torsion angles in a β-chain are plotted as a function of time in Fig. 4. The lifetimes of *trans* conformations are 3–4 times longer than the lifetimes of *gauche* conformations. As expected, their proportion is the same as for the populations of *trans* and *gauche* states. The lifetimes decrease towards the end of the alkyl chain and also show some oscillations.

Table 1. The probabilities of *gauche*$^+$ (g^+), *gauche*$^-$ (g^-) and *trans* conformations along the β-, γ- and α-chain in the DMPC bilayer membrane. The sums of the probabilities of g^+ and g^- ($g^+ + g^-$) and their standard deviations (S.D.) are also given

Conformation	β-Chain					γ-Chain				
torsion No.	g^+	g^-	*trans*	$g^+ + g^-$	S.D.	g^+	g^-	*trans*	$g^+ + g^-$	S.D.
4	0.06	0.12	0.80	0.18	0.026	0.07	0.05	0.85	0.13	0.035
5	0.10	0.14	0.74	0.24	0.043	0.14	0.12	0.73	0.25	0.041
6	0.08	0.11	0.79	0.19	0.041	0.09	0.07	0.83	0.16	0.041
7	0.11	0.08	0.80	0.18	0.042	0.11	0.11	0.76	0.22	0.033
8	0.11	0.14	0.74	0.24	0.045	0.11	0.09	0.78	0.20	0.035
9	0.09	0.10	0.78	0.20	0.037	0.10	0.12	0.76	0.22	0.034
10	0.10	0.10	0.78	0.20	0.040	0.10	0.11	0.77	0.22	0.041
11	0.12	0.14	0.73	0.25	0.043	0.11	0.12	0.75	0.23	0.037
12	0.10	0.12	0.77	0.21	0.038	0.11	0.09	0.78	0.21	0.030
13	0.10	0.11	0.77	0.21	0.045	0.12	0.14	0.72	0.26	0.044
14	0.12	0.13	0.73	0.25	0.035	0.11	0.11	0.76	0.22	0.034
α-Chain										
1	0.40	0.38	0.14	0.78	0.029					
2	0.27	0.21	0.12	0.48	0.036					
3	0.30	0.26	0.21	0.56	0.037					
4	0.07	0.08	0.76	0.14	0.032					
5	0.08	0.07	0.81	0.16	0.036					
θ-Torsion										
1	0.00	0.00	0.98	0.01	0.007					

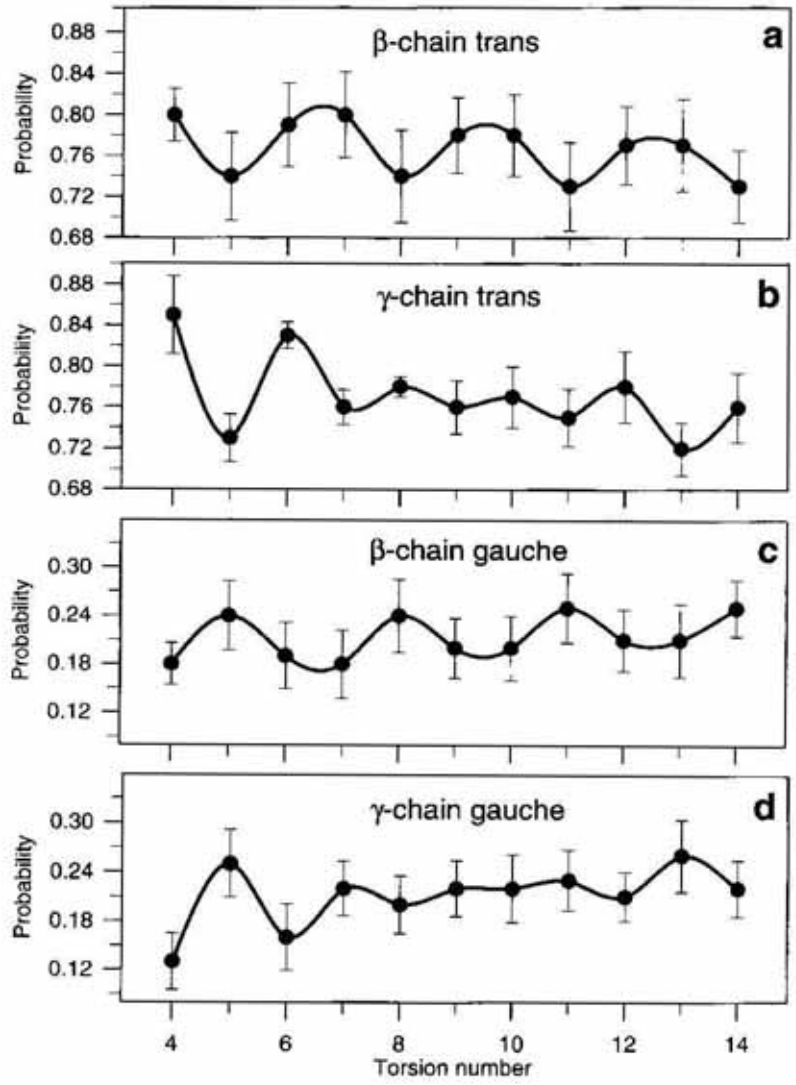

Figure 2. The probabilities of conformations along the hydrocarbon chains.

(**a**) *Trans* and (**c**) *gauche* conformations for the β-chain. (**b**) *Trans* and (**d**) *gauche* conformations for the γ-chain. Error bars indicate the standard deviations.

It is interesting to notice in Fig. 4 that transitions between any two states are very fast — they occur in a time shorter than the time step of 1 ps. Also, that the torsion angles reside mainly in well defined conformational states (i.e., between the dashed lines in Fig. 4); intermediate conformations are rare and their lifetimes are very short (Fig. 4).

Average tilt of hydrocarbon chains

In the DMPC bilayer in the crystalline phase (which is the initial structure in MD simulation) all hydrocarbon chains have the same orientation and conformation, and the tilt angle of chains with respect to the bilayer normal is 17.9° [11]. The tilt angle of hydrocarbon chains in the fully hydrated liquid-crystalline PC bilayer is known experimentally to be zero [20, 22] and this is also the theoretical prediction [23]. The tilt angle of chains is found to be near zero (6.5°) in the computer simulated membrane after equilibration. This indicates that the mean orientations of the chains relative to the normal are almost randomly distributed within a cone. The cone angle corresponds to the largest tilt angle. Figure 5a shows the distributions of tilt angles for γ-chains. Both for the β- and the γ-chain the largest tilt angle is about 65°. The distributions of mean orientations of the γ-chains in the *x,y*-plane are shown in Fig. 5b. The orientations cover the whole range of angles (0–360°). The non-zero tilt of 6.5°, obtained after averaging over orientations and time, might have resulted from a too short averaging time (of 2500 ps) compared to the time of *trans-gauche* isomerisation (see Table 2) and rotational diffusion of chains (see below, Table 4). Again, it might

Table 2. The periods of transitions between *trans* (t) and *gauche* (g) conformations in the α-, β-, and γ-chain in the DMPC bilayer

	β-Chain			γ-Chain		
Transition	t → g	g → t	g → g	t → g	g → t	g → g
Torsion No.	[ps]	[ps]	[ps]	[ps]	[ps]	[ps]
1	763	760	60000			
4	375	370	27000	340	346	54000
5	245	241	5143	225	224	7714
6	316	323	15429	378	376	12000
7	310	310	18000	293	295	7200
8	294	298	6000	336	336	18000
9	299	296	13500	298	294	6000
10	277	282	8308	289	292	12000
11	273	270	6000	262	260	13500
12	235	238	13500	252	250	10800
13	213	210	5400	200	197	5143
14	163	165	7714	184	184	4909
α-Chain						
1	923	947	none			
2	529	528	3103			
3	134	134	790			
4	154	156	45000			
5	254	252	36000			
θ-Torsion						
1	11250	10588	none			

have resulted from a too small number of DMPC molecules in the simulated bilayer (72 DMPC molecules), compared to the number of molecules in model membranes studied experimentally.

Rotational diffusion of chains

Reorientational autocorrelation functions (RAF) (cf. Eqn. 1) were calculated for the β- and γ-chain vectors. The β-chain vector is defined as a vector linking the middle of C21–C22 bond with the centre of gravity of the β-chain, and the γ-chain vector as a vector linking the middle of C32–C34 bond with the centre of gravity of the γ-chain. Autocorrelation functions were calculated for the Legendre polynomials $P_1(\cos\theta) = \cos\theta$, and $P_2(\cos\theta) = 0.5 \times (3\cos^2\theta - 1)$, where θ is the angle between $\mathbf{n}(t_0)$ and $\mathbf{n}(t_0 + t)$, $\mathbf{n}$ is the β- or γ-chain vector, and t_0 is the initial time. The RAF's were averaged over 500 initial times t_0. The time constants were obtained from the RAF's according to equation 2 in the

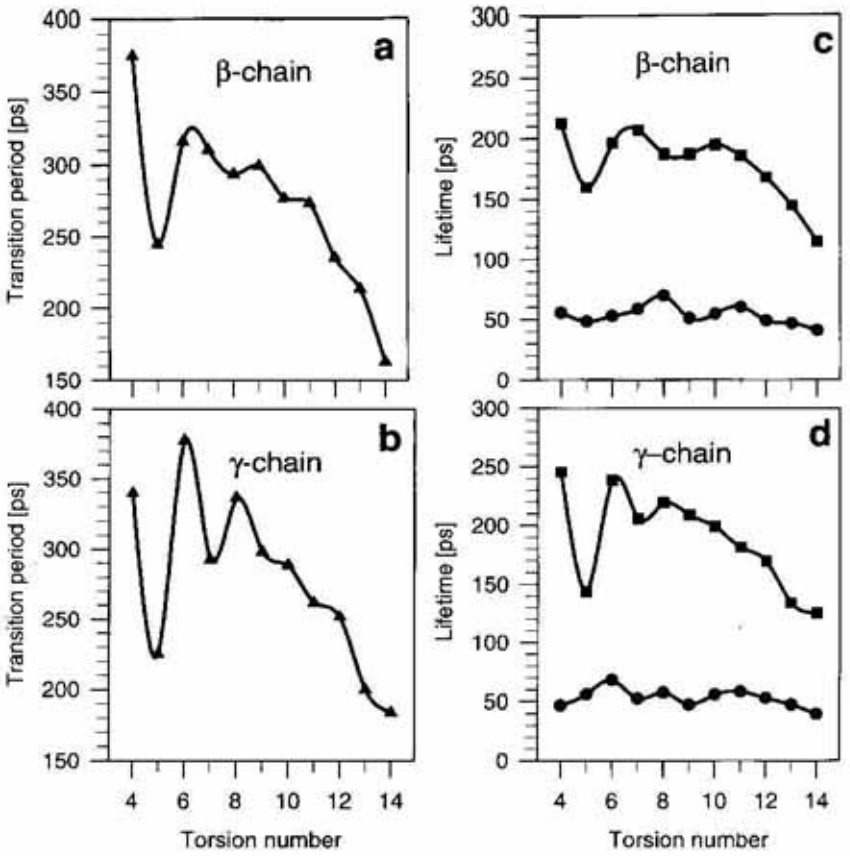

Figure 3. The transition periods for *trans* → *gauche* transitions along the β-chain (a) and γ-chain (b).

The lifetimes for *trans* (solid squares) and *gauche* (solid circles) conformations along the β-chain (**c**) and γ-chain (**d**).

region of 2000 ps. Figure 6a and b show RAF's for P_1 and P_2 for the β-chain vector together with their fits. The best fit parameters are given in Table 4. As can be seen, the decays of RAF's occur mainly through a single mechanism with a correlation time of the order of 10^{-8} s. Such a long correlation time indicates that, in spite of a relatively fast intra-chain motion, due to *trans-gauche* isomerisation, the "rigid body" rotation of chains is slow.

Molecular order parameter, S_{mol}

The order parameter, S_{mol}, describes the average orientation of the (C_{n-1}, C_{n+1}) vector, linking two (n–1 and n+1) carbon atoms in the hydrocarbon chain, relative to the membrane normal. S_{mol} ranges from 1.0 for all-*trans* conformation of chains and tilt angle equal to zero, to –0.5, for all chains perpendicular to the bilayer normal, and is zero when orientations of chains' segments are random in the range (–90°, 90°). Averaging is over both the ensemble and the time. The profiles of the order parameter for β- and γ-chain for the simulated DMPC bilayer are shown in Fig. 7. The corresponding order parameters lie within the range of each other's errors so that the profiles for β- and γ-chain do not differ significantly.

In the case of the alkyl chain, the value of the order parameter for a given segment is determined both by the *trans-gauche* isomerisation within the segment and within all segments above it, and by the "rigid body" rotation of the chain about the in-plane axis (so called perpendicular axis) [24]. The effect of rotational isomerism is cumulative — "disorder" i.e., departure from the parallel orientation of the chain segment to the membrane normal, increases along the chain, while the effect of the "rigid body" rotation is constant along the chain. It is, however, practically impossible to separate these two effects from each other.

α-Chain

Conformations

In the DMPC single crystal structure (Fig. 1) the conformation of the head group α-chain

Table 3. The lifetimes of conformations in the α-, β-, and γ-chain in the DMPC bilayer

	β-Chain			γ-Chain		
Conformation	g^+	g^-	t	g^+	g^-	t
Torsion No.	[ps]	[ps]	[ps]	[ps]	[ps]	[ps]
4	56	68	212	47	41	245
5	48	57	160	56	46	144
6	53	59	196	68	51	239
7	59	50	207	52	59	205
8	70	62	187	57	60	219
9	51	57	187	47	77	209
10	55	55	195	56	68	199
11	60	64	185	58	62	181
12	49	54	168	53	51	170
13	47	46	144	47	48	134
14	41	41	114	39	42	125
α-Chain						
1	404	308	100			
2	172	125	60			
3	57	59	27			
4	19	24	106			
5	34	34	162			
θ-Torsion						
1	78	28	757			

is such that the α2, α3, and α5 torsions are *gauche*; α1 and α4 torsions are *trans* (Fig. 1 and [11]). In the simulated DMPC bilayer in the liquid-crystalline phase the conformation of α1 changes to predominantly *gauche* and that of α5 to *trans* (Table 1 and Fig. 8). α2 and α3 remain mainly *gauche*, however, the conformations of about 52% of α2 and 23% of α3 are not well defined. a4 remains mainly *trans* (Table 1 and Fig. 8). Consecutive conformations of α2 and α3 are mainly g^+,g^- (42%), g^-,g^- (36%) and *trans*,g^- (18%), i.e., such, that α3 is g^- and α2 is mainly *gauche*.

Transitions between conformations

The average periods for the transitions *trans* → *gauche*, *gauche* → *trans* and *gauche* → *gauche* along the α-chain are given in Table 2. *Trans* → *gauche* and *gauche* → *trans* transitions of α1 are rare, with an average transition period of about 1 ns, while *gauche* → *gauche* did not take place during 2.5 ns. Thus, α1 is either g^+ or g^-. *Trans* → *gauche* transitions for α4 and α5 have similar periods as those in the hydrocarbon chains. α2 resides in *gauche* conformation in 48% of

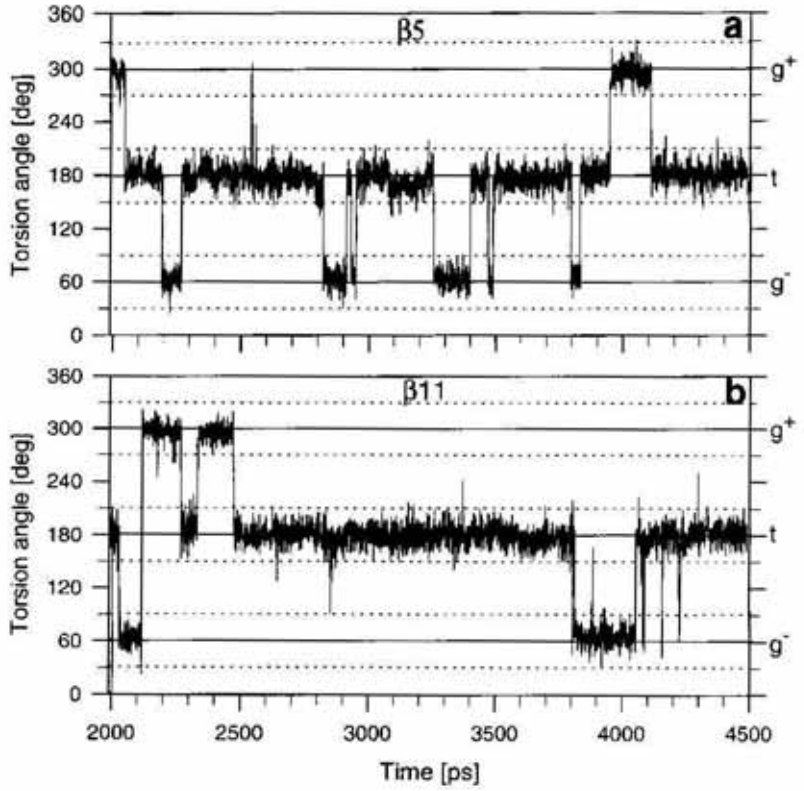

Figure 4. The conformations of two arbitrary selected torsion angles in a β-chain as a function of time.

Trans, *gauche*$^+$ and *gauche*$^-$ are marked on the right hand side as t, g^+ and g^-, respectively. The dashed lines indicate the ranges of angles characterising a given conformation.

cases, while in 52% of cases its conformation is not well defined (Fig. 8). It is, therefore, difficult to determine precisely when *trans* → *gauche* transitions really do occur although certainly they are not frequent. In the case of α3, whose conformational state is better defined, transitions between conformations are the most frequent of all torsion angles considered.

The lifetimes of conformation states along the α-chain are given in Table 3. The ratios of the lifetimes of *trans* and *gauche* conformations along the α-chain reflect the ratios of populations of the states.

Conformation and transitions of θ1

In both conformations of DMPC in the single crystal structure, the C1–C2 bond constitutes the rotation axis for the motion of the phosphorylcholine moiety [25]. In the liquid-crystalline phase, the rotation around the C1–C2 axis is hindered [26, 27]. In the computer model DMPC bilayer the conformation of θ1 (see Fig. 1) torsion is firmly *trans* (Fig. 8 and Table 1) and *trans* → *gauche* and *gauche* → *trans* transitions are very rare — on average they occur every 11 ns (Table 2). So that, in this model, the head group rotation calculated below cannot take place around the C1–C2 bond.

Rotational diffusion of the head group

The reorientational autocorrelation function (cf. Eqn. 1) of the vector linking the phosphorus and nitrogen atoms of the phosphorylcholine group (P–N vector) is a measure of the head group rotational motion. Figure 6c and d show the RAF's for the P_1 and P_2 Legendre polynomial for the P–N vector together with their fits. The best fit parameters are given in Table 4. The decay of the RAF occurs predominantly by way of a single mechanism with relatively long correlation times: 7.5 ns for P_1 and 3.7 ns for P_2. As can be seen from Table 2, the transition times between conformations for θ1, α1 and α2 torsions are too slow to be responsible for the P–N vector rotation. The rotation is therefore a result of a combined effects of the α3, α4 and α5 isomerisation. The effect on the "rigid body" motion of the *trans-gauche* isomerisation in the α-chain is much stronger than that in the hydrocarbon chains. This is probably because the α-chain is much shorter and has

Table 4. The rotational correlation times for the rotations of the β-chain and γ-chain vectors, the P–N vector and the O21–C1 vector

P_1	β-Chain	γ-Chain	P–N	O21-C1
decay:				
1: Time [ps]	308	210	200	190
Amplitude	0.02	0.01	0.06	0.03
2: Time [ps]	36000	48800	922	770
Amplitude	0.98	0.98	0.06	0.04
3: Time [ps]			7570	17900
Amplitude			0.87	0.91
4: Time [ps]				
Amplitude				
P_2				
decay:				
1: Time [ps]	413	440	11	10
Amplitude	0.09	0.08	0.04	0.04
2: Time [ps]	15000	35000	125	220
Amplitude	0.91	0.92	0.08	0.05
3: Time [ps]			465	690
Amplitude			0.16	0.13
4: Time [ps]			3770	7120
Amplitude			0.70	0.74

two bulky groups (the phosphate and choline groups) which significantly lower its internal flexibility.

DMPC molecule

The results presented above indicate that rotational motion of the hydrocarbon chains is separated from that of the head group in the DMPC molecule. In this paragraph, the translational and rotational motions of the whole DMPC molecule are calculated.

The diffusion coefficients for DMPC self-diffusion in the membrane, in the *x,y*-plane of the membrane and along the *z*-axis, were obtained by calculating the respective mean square displacements (MSD) (cf. Eqn. 3) of the centre of mass of the DMPC molecule. In each case, MSD was averaged over 1000 initial times. The rotational correlation times were obtained by calculating the RAF (cf. Eqn. 1) for the vector linking C1 and O21 atoms (see Fig. 1). This vector was chosen because *trans-gauche* isomerisations of β1, θ1 and α1 are very slow (Table 2) and, to a large extent, the rotation of this vector represents that of the whole molecule.

Translational diffusion

The diffusion coefficients were calculated from the linear part of the MSD curves (Fig. 9) according to Eqn. 4. The diffusion coefficients for translational self-diffusion of DMPC molecules in the membrane (D), in the plane of the membrane ($D_{||}$) and along the

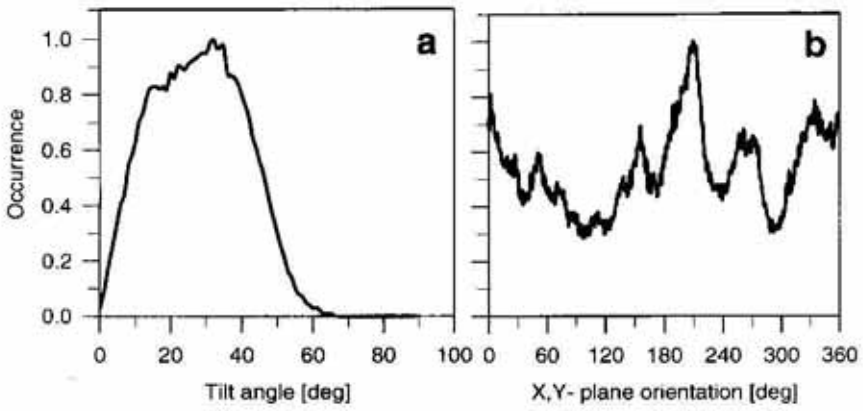

Figure 5. (a) The distribution of tilt angles for γ-chains. (b) The distribution of mean orientations of the γ-chains in the *x,y*-plane.

normal (D⊥) are practically the same: $D = D_{||} = D_{\perp} = 2.0 \times 10^{-7}$ cm^2/s. Apparently, both lateral and transversal diffusion takes place in the membrane and at the same rate. Trajectories of the centre of mass of an arbitrarily chosen DMPC molecule, shown in Fig. 10, illustrate the motion of DMPC in the *x,y*- and *x,z*-plane.

Rotational diffusion

Figure 6e and f show the RAF's for P_1 and P_2 for the O21–C1 vector (shoulder vector) together with their fits. The best fit parameters are given in Table 4. The decay of the RAF occurs mainly through a mechanism with a correlation time of about 18 ns for P_1 and 7.0 ns for P_2. The decay of the RAF of the projection of the shoulder vector on the *x,y*-plane is faster by more than a factor of two than that of the projection on the *z*-axis (not shown). This, together with the fact that the projection of the shoulder vector on the *z*-axis (the molecule long axis) is close to zero, may indicate that either the shoulder vector constitutes the rotation axis for the fluctuations of the long axis, or the "rigid body" rotation of the DMPC molecule around the perpendicular axis does not take place.

DISCUSSION

The results of computer simulation of a dimyristoylphosphatidylcholine (DMPC) bilayer membrane in water are presented. The data obtained in this calculation provide a very detailed picture of structural and dynamic properties to be expected of the DMPC molecule. A preliminary comparison of these results and some experimental results is presented below.

Conformations of hydrocarbon chains and conformational transitions

The number of *gauche* conformations per hydrocarbon chain in the simulated DMPC bilayer was found to be 2.8 ± 0.1, in good agreement with experimental estimates [1, 2]. Experimental results suggest that the probability of a *gauche* conformation is not uniform along the chain, but increases towards the terminal methyl group [20, 21, 28]. The results of the simulation show that the probability of a *gauche* conformation varies periodically along the chain (in the β-chain higher probability is at every third CH_2 group while in the γ-chain it is at every other CH_2 group) with only a slight increase towards the end of the chain. However, the frequency of transitions between conformations increases, by more than a factor of two along the chain, and shows some periodic features. The increase in the transition frequency is mainly associated with a decrease in the lifetime of the *trans* conformation along the chain, as the lifetime of the *gauche* conformations does not decrease significantly. Both lifetimes do, however, exhibit periodic oscillations. The results of MD simulation indicate, therefore, that the "flexibility gradient" in the hydrocarbon chains is related to the decreasing lifetime of the *trans* conformation along the chain and not to an increasing probability of the *gauche* conformation. The periodic character of probability of the conformational states seems to indi-

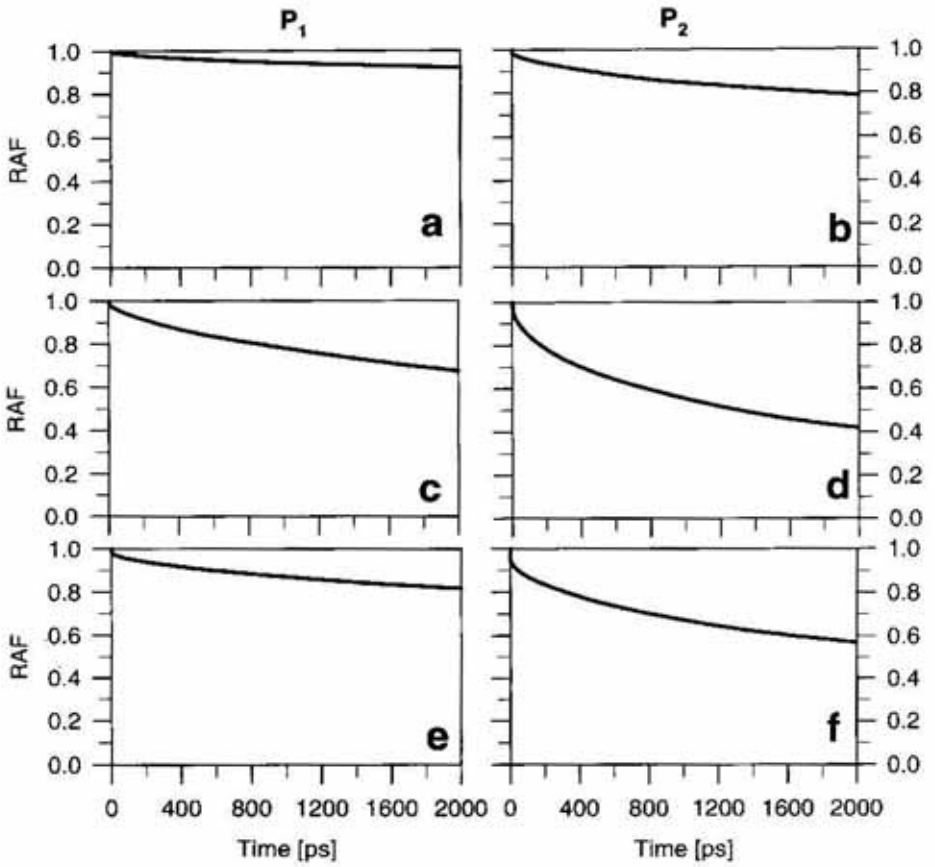

Figure 6. The reorientational autocorrelation functions (RAF) for the first (P_1) and second (P_2) Legendre polynomials.

The RAF's for P_1 and P_2 are, respectively: (**a**) and (**b**) for the β-chain vector; (**c**) and (**d**) for the P–N vector; (**e**) and (**f**) for O21–C1 vector. Each curve was averaged over 500 initial times. To obtain the time constants each RAF was fitted with a sum of two- to four-exponential decay function. The fitted lines are superimposed on the respective RAF's.

cate that a repeating |*-trans-trans-gauche-*| conformation for the β-chain between the 6th and 14th torsion angle might be more likely than a |*-trans-trans-trans-*| conformations. For the γ-chain the likely conformation along the whole chain is |*-trans-gauche-*|, although in both chains *trans* conformation of each torsion is at least 3 times more probable than that of *gauche*. These results are consistent with the predicted low probability of *-gauche-gauche-* conformations in alkyl chains in the membrane.

The lifetimes of conformations in the alkyl chains have been found to be in the range of $1–2 \times 10^{-10}$ s for *trans* conformations and in the range of $4–7 \times 10^{-11}$ s for *gauche* conformations, while the *trans* → *gauche* transition periods are in the range of $1.6–3.8 \times 10^{-10}$ s. Experimentally determined correlation times for *trans-gauche* isomerism are somewhat ambiguous: Seelig & Gally [29] and Meier *et al.* [8] give a value of 10^{-10} s, while Moser *et al.* [20] a value in the range $1–16 \times 10^{-12}$ s. The lifetimes and transition periods cannot be directly compared with the correlation times, however all the values are within the same range.

α-Chain conformation

In the simulated DMPC bilayer α5 is *trans* in 81% and *gauche* in 15% of cases. This is in general agreement with the result of another molecular dynamics simulation of a hydrated DMPC bilayer [30] as well as with experimental results of Yeagle *et al.* [31, 32] and of Griffin *et al.* [33]. Our result is at variance with the interpretation of the experimental results of Hauser *et al.* [34] and Akutsu [35]. However, the experiments described in the latter papers were performed only on phospholipids in a monomeric form or in small micelles, so their results may not be applicable to the bilayer structures.

Trans conformation of α5 is associated with an extended, rather than bent, conformation of the α-chain of the PC head group. This facilitates the formation of intermolecular charge-pairs between the positively charged choline and negatively charged phosphate

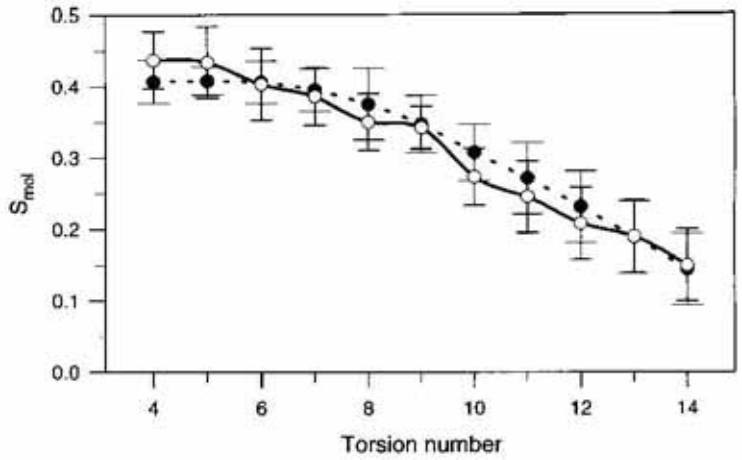

Figure 7. The profiles of the molecular order parameter (S_{mol}) calculated for β-chain (solid circles and dashed line) and γ-chain (open circles and solid line).

Error bars indicate the standard deviations; for the β-chain the horizontal bars are longer than those for the γ-chain.

groups, suggested by Nagle [36] and observed in the liquid-crystalline phase both experimentally [32, 37] and in a computer model (Pasenkiewicz-Gierula, M., unpublished).

Rotation of the P–N vector

Experimentally measured rotational correlation times of the P–N vector at a temperature 10°C above the main transition temperature for dipalmitoylPC (DPPC) (16-carbon atoms chains) is 2.3 ns [38] and for eggPC (EPC) at 23°C it is 1.4 ns [31]. In the simulated DMPC bilayer membrane at a temperature about 14°C above the main phase transition temperature, the rotational correlation time for P_2 is 3.7 ns. Rotational motion of the P–N vectors in DMPC, DPPC and EPC should be similar since DMPC differs from DPPC and EPC only in the length and

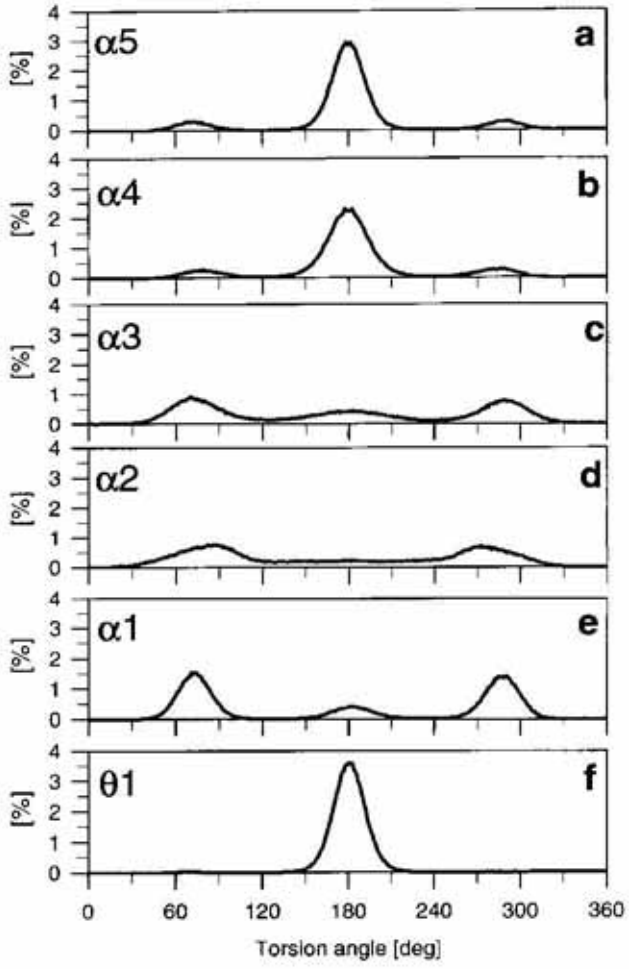

Figure 8. The populations of the torsion angles from the α-chain and of the θ1 torsion.

The torsion angles are marked on the left hand side of the Figure. Angles around 60°, 180°, 300° correspond to *trans*, *gauche*$^+$, and *gauche*$^-$ conformations, respectively.

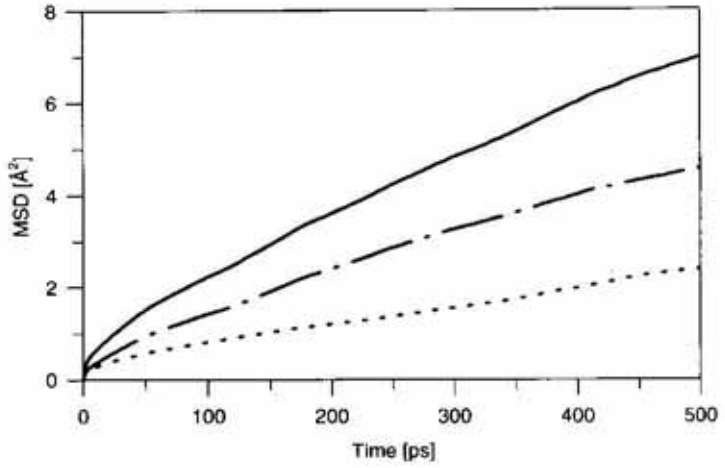

Figure 9. The mean square displacements (MSD) of the centre of mass of the DMPC molecule in the membrane (solid line), in the *x,y*-plane of the membrane (dash-dot line) and along the *z*-axis (doted line).

Each curve was averaged over 1000 initial times. The diffusion coefficients were calculated from the linear parts of MSD's.

number of saturated bonds in the alkyl chains. The value obtained in the simulation can be considered as being close to the values obtained experimentally, if the uncertainty in determining the rotational correlation times is taken into account. The results of the simulation indicate that C2–C1 bond cannot constitute the rotation axis for the P–N vector rotation because inter-conformational transition periods for α1 and θ1 are too long. Although such a model was originally proposed by Hauser *et al.* [34] and Seelig *et al.* [27] it was later undermined by new experimental evidence [26]. Simulation shows that P–O12 (α3) and O12–C11 (α4) bonds are possible candidates for the rotation axes.

The observed *gauche-gauche* conformation of the phosphodiester linkage (α2–α3), resulting in a bend of the phosphorylcholine moiety at the position of the phosphate group, is in good agreement with experimental data [27]. In the simulated membrane the most frequent conformations of α2-α3 are those where α3 is g^- while α2 is either g^+ or g^-.

Translational diffusion of DMPC in the membrane

The lateral self-diffusion coefficient has been determined as $1.8 \pm 0.6 \times 10^{-8}$ cm^2/s for didihydrosterculoylPC in a membrane at 25°C [5], and as 3.6×10^{-8} cm^2/s for DMPC in a membrane at 21°C [39]. Lateral diffusion coefficients of *N*-(7-nitro-2,1,3-benzoxadiazol-4-yl)phosphatidylethanolamine in PC membranes as a function of temperature and membrane composition were determined to be of the order of 1×10^{-7} cm^2/s at a temperature above 35°C. In the simulated DMPC bilayer membrane at 37°C, the lateral self-diffusion coefficient is 2×10^{-7} cm^2/s and so is in a good agreement with the experimental data. The simulation shows that the diffusion coefficient for lateral and transverse diffusion is similar, although transverse diffusion takes place only over a limited range of vertical distances due to the balance between hydrophobic and hydrophilic interactions of PC molecules and water, whereas lateral diffusion is not distance-limited.

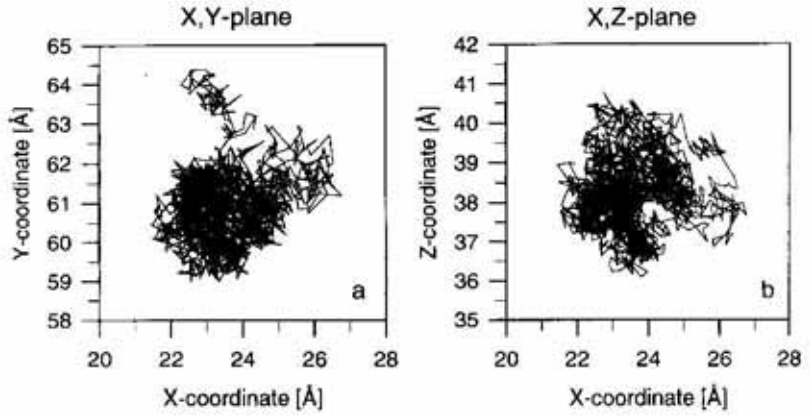

Figure 10. The trajectory of the centre of mass of an arbitrarily chosen DMPC molecule in (a) the *x,y*-plane and (b) *x,z*-plane.

Rotational diffusion of DMPC in the membrane

"Rigid body" rotational motion of the four main segments of DMPC (that is the α- β- and γ-chains and the glycerol group) is represented by the decays of RAF's for the β-chain, γ-chain, P–N, and O21–C1 vectors. The slowest decay for P_2 is that for the alkyl chains, with the correlation times of 15 and 35 ns for the β- and γ-chain, respectively. The fastest is 3.8 ns for the P–N vector. The correlation time for the O21–C1 vector is about 7.0 ns. These results of the simulation might suggest that, in the liquid-crystalline bilayer, there is no rotation of the DMPC molecule as a whole and each segment of the molecule exhibits its own rotational freedom, in addition to its internal flexibility resulting from rotational isomerism.

It will be difficult to verify this conclusion experimentally because there are no means of measuring independently the rotational correlation time for the whole PC molecule in the membrane. As discussed above, the experimentally determined correlation times for the P–N vector rotation in the plane of the membrane are 1.4 ns [31] and 2.3 ns [38]. The correlation times for the hydrocarbon chains rotation around the long axis and around the in-plane axis, range from 1.2 to about 100 ns [20]. Thus the range of correlation times seems to be broad for making any meaningful comparison.

REFERENCES

1. Casal, H.L. & McElhaney, R.N. (1990) Quantitative determination of hydrocarbon chain conformational order in bilayers of saturated phosphatidylcholines of various chain lengths by Fourier transform infrared spectroscopy. *Biochemistry* **29**, 4523–5427.
2. Mendelsohn, R., Davies, M.A., Brauner, J.W., Schuster, H.F. & Dluhy, R.A. (1989) Quantitative determination of conformational disorder in the acyl chains of phospholipid bilayers by infrared spectroscopy. *Biochemistry* **28**, 8934–8939.
3. Maroncelli, M., Qi, S.P., Strauss, H.L. & Snyder, R.G. (1982) Nonpolar conformers and the phase behavior of solids n-alkanes. *J. Am. Chem. Soc.* **104**, 6237–6247.
4. Wang, C.C. & Pecora, R. (1980) Time-correlation function for restricted rotational diffusion. *J. Chem. Phys.* **72**, 5333–5336.
5. Devaux, P. & McConnell, H.M. (1972) Lateral diffusion in spin-labeled phosphatidylcholine multilayers. *J. Am. Chem. Soc.* **94**, 4475–4481.
6. Vaz, W.L.C., Clegg, R.M. & Hallmann, D. (1985) Translational diffusion of lipids in liquid crystalline phase phosphatidylcholine multibilayers. A comparison of experiment with theory. *Biochemistry* **24**, 781–786.
7. Sackmann, E. (1995) Physical basis of self-organization and function of membranes: Physics of vesicles; in *Structure and Dynamics of Membranes* (Lipowsky, R. & Sackmann, E., eds.) pp. 213–304, Elsevier, Amsterdam.
8. Meier, P., Ohmer, E. & Kothe, G. (1986) Multipulse dynamic nuclear magnetic resonance of phospholipid membranes. *J. Chem. Phys.* **85**, 3598–3614.
9. Weisz, K., Gröbner, G., Mayer, C., Stohrer, J. & Kothe, G. (1992) Deuteron nuclear magnetic resonance study of the dynamic organization of phospholipid/cholesterol membranes: Molecular properties and viscoelastic behavior. *Biochemistry* **31**, 1100–1112.
10. Pearlman, D.A., Case, D.A., Caldwell, J.C., Seibel, G.L., Singh, U.C., Weiner, P.K. & Kollman, P.A. (1991) *AMBER 4.0.* University of California, San Francisco.
11. Vanderkooi, G. (1991) Multibilayer structure of dimyristoylphosphatidyl-choline dihydrate as determined by energy minimization. *Biochemistry* **30**, 10760–10768.
12. Pasenkiewicz-Gierula, M., Takaoka, Y., Miyagawa, H., Kitamura, K. & Kusumi, A. (1997) Hydrogen bonding of water to phosphatidylcholine in the membrane as studied by a molecular dynamics simulation: Location, geometry, and lipid-lipid bridging *via* hydrogen-bonded water. *J. Phys. Chem.* (in press).
13. Jorgensen, W.L. & Tirado-Rives, J. (1988) The OPLS potential functions for proteins. Energy minimization for crystals of cyclic peptides

and crambin. *J. Am. Chem. Soc.* **110**, 1657–1666.

14. Jorgensen, W.L., Chandrasekhar, J., Madura, J.D., Impey, R. & Klein, M.L. (1983) Comparison of simple potential functions for simulating liquid water. *J. Chem. Phys.* **79**, 926–935 (and references therein).

15. Ryckaert, J.P., Cicotti, G. & Berendsen, H.J.C. (1977) Numerical integration of the Cartesian equations of motion of a system with constraints: molecular dynamics of n-alkanes. *J. Comp. Phys.* **22**, 327–341.

16. Egberts, E., Marrik, S.-J. & Berendsen, H.J.C. (1994) Molecular dynamics simulation of a phospholipid membrane. *Eur. Biophys. J.* **22**, 432–436.

17. Berendsen, H.J.C., Postma, J.P.M., van Gunsteren, W.F., DiNola, A. & Haak, J.R. (1984) Molecular dynamics with coupling to an external bath. *J. Chem. Phys.* **81**, 3684–3690.

18. Pearson, R.H. & Pascher, I. (1979) The molecular structure of lecithin dihydrate. *Nature* (London) **281**, 499–501.

19. Pink, D.A., Green, T.J. & Chapman, D. (1980) Raman scattering in bilayers of saturated phosphatidylcholines. Experiment and theory. *Biochemistry* **19**, 349–356.

20. Moser, M., Marsh, D., Meier, P., Wassmer, K.-H. & Kothe, G. (1989) Chain configuration and flexibility gradient in phospholipid membranes. *Biophys. J.* **55**, 111–123.

21. Hubbell, W.L. & McConnell, H.M. (1971) Molecular motion in spin-labeled phospholipids and membranes. *J. Am. Chem. Soc.* **93**, 314–326.

22. Meier, P., Blume, A., Ohmes, E., Neugebauer, F.A. & Kothe, G. (1982) Structure and dynamics of phospholipid membranes: An electron spin resonance study employing biradical probes. *Biochemistry* **21**, 526–534.

23. Carlson, J.M. & Sethna, J.P. (1987) Theory of the ripple phase in hydrated phospholipid bilayers. *Phys. Rev. A* **36**, 3359–3374.

24. Pastor, R.W., Venable, R.M. & Karplus, M. (1988) Brownian dynamics simulation of a lipid chain in a membrane bilayer. *J. Chem. Phys.* **89**, 1112–1127.

25. Hauser, H., Pascher, I., Pearson, R.H. & Sundell, S. (1981) Preferred conformation and molecular packing of phosphatidylethanolamine and phosphatidylcholine. *Biochim. Biophys. Acta* **650**, 21–51.

26. Büldt, G. & Wohlgemuth, R. (1981) The headgroup conformation of phospholipids in membranes. *J. Membr. Biol.* **58**, 81–100.

27. Seelig, J., Gally, H.-U. & Wohlgemuth, R. (1977) Orientation and flexibility of the choline head group in phosphatidylcholine bilayers. *Biochim. Biophys. Acta* **467**, 109–119.

28. Allegrini, P.R., Scharrenburg, G, Haas, G.H. & Seelig, J. (1983) ^{2}H- and ^{31}P-NMR studies of bilayers composed of 1-acyllysophosphatidylcholine and fatty acids. *Biochim. Biophys. Acta* **731**, 448–455.

29. Seelig, J. & Gally, H.U. (1976) Investigation of phosphatidylethanolamine bilayers by deuterium and phosphorus-31 nuclear magnetic resonance. *Biochemistry* **15**, 5199–5204.

30. Robinson, A.J., Richards, W.G., Thomas, P.J. & Hann, M.M. (1994) Head group and chain behavior in biological membranes: A molecular dynamics computer simulation. *Biophys. J.* **67**, 2345–2354.

31. Yeagle, P.L., Hutton, W.C., Huang, C-h. & Martin, R.B. (1975) Headgroup conformation and lipid-cholesterol association in phosphatidylcholine vesicles: A ^{31}P{^{1}H} nuclear Overhauser effect study. *Proc. Nat. Acad. Sci. U.S.A.* **72**, 3477–3481.

32. Yeagle, P.L., Hutton, W.C., Huang, C-h. & Martin, R.B.(1976) Structure in the polar head group region of phospholipid bilayers: A ^{31}P {^{1}H} nuclear Overhauser effect study. *Biochemistry* **15**, 2121–2124.

33. Griffin, R.G., Powers, L. & Pershan, P.S. (1978) Head-group conformation in phospholipids: A phosphorus-31 nuclear magnetic resonance study of oriented monodomain dipalmitoyl-phosphatidylcholine bilayers. *Biochemistry* **17**, 2718–2722.

34. Hauser, H., Guyer, W., Skrabal, P. & Sundell, S. (1980) Polar group conformation of phosphatidylcholine. Effect of solvent and aggregation. *Biochemistry* **19**, 366–373.

35. Akutsu, H. (1981) Direct determination by Raman scattering of the conformation of the choline group in phospholipid bilayers. *Biochemistry* **20**, 7359–7366.

36. Nagle, J.F. (1976) Theory of lipid monolayer and bilayer phase transitions: Effect of headgroup interactions. *J. Membr. Biol.* **27**, 233–250.

37. Yeagle, P.L., Hutton, W.C., Huang, C-h. & Martin, R.B. (1977) Phospholipid head-group conformations; Intermolecular interactions and cholesterol effects. *Biochemistry* **16**, 4344–4349.

38. Shepherd, J.C. & Büldt, G. (1978) Zwitterionic dipoles as dielectric probe for investigating head group mobility in phospholipid membranes. *Biochim. Biophys. Acta* **514**, 83–94.

39. Schindler, H. & Seelig, J. (1973) EPR spectra of spin labels in lipid bilayers. *J. Chem. Phys.* **59**, 1841–1850.